Original Article

Adsorption investigation of a composite of metal-organic framework and polyethylene oxide hydrogel

Emmanuel B AttahDaniel[1], Ezekiel D Dikio[2], Nimibofa Ayawei[3],
Donbebe Wankasi[2], Fanyana M Mtunzi[1] and
Paul N Diagboya[1] (iD)

Abstract

Though adsorption techniques are eco-environmentally friendly, most lack the effectiveness of complete contaminant elimination leading to increasing concerns about the presence of aqueous contaminants on humans. Thus, synergistic combination of low adsorption capacity adsorbents may be an effective method to enhance their aqueous contaminant uptake. Sol-gel synthesized lanthanum-1,4-benzene dicarboxylate metal organic framework (LaBDC MOF) and polyethylene oxide (PEO) hydrogel were combined to prepare a synergistic composite adsorbent (PEO-LaBDC) for aqueous methylene blue (MB) adsorption. Major properties of the pristine LaBDC MOF and PEO hydrogel were expressed in the characterized composite indicating successful preparation. PEO-LaBDC composite MB removal rate of MB was at least twice as fast (60 min) to those of the pristine LaBDC MOF (120 min) and PEO hydrogel (125 min). The fitting of kinetics model was fractal in nature, and optimum adsorption was on the alkaline end of the pH spectrum for all adsorbents (pH = 12, 10, and 10, respectively). Comparatively, the composite exhibited a better adsorption performance of $\approx 177\%$ higher than the pristine LaBDC MOF; buttressing the idea that synergistic combination of adsorbents in composites could enhance adsorption processes. Therefore, the PEO-LaBDC composite is a promising adsorbent for the remediation of aqueous MB.

Introduction

Water pollution resulting from untreated and poorly treated industrial effluents is a major issue as a significant global population ($\geq 33\%$) lack reliable access to clean water for use due to contamination.[1,2] Dye accounts for almost a third of the contamination menace globally.[3] The structure of most dyes makes them teratogenic, mutagenic, known carcinogens, harmful to health, causing human respiratory and eye irritations, causing suffocation via formation of methemoglobin, a distorted form of hemoglobin which lacks the ability to bind oxygen, and ultimately death.[4] Thus, the need for enhanced treatment techniques cannot be over-emphasized.

Several techniques including oxidation, photocatalysis, membrane separation, adsorption, ion exchange, electrochemical techniques, and reverse osmosis have been employed for contaminated water treatment.[5,6] Adsorption technique presents better merits than most others in that it is cheap and environmentally friendly

with high stability and mechanical strength, easy to regenerate and reuse, can be configured for specific

[1]Environmental Fate of Chemicals and Remediation Laboratory, Department of Biotechnology and Chemistry, Vaal University of Technology, Vanderbijlpark, Gauteng, South Africa
[2]Department of Chemical Sciences, Faculty of Sciences, Niger Delta University, Wilberforce Island, Nigeria
[3]Department of Chemistry, Bayelsa Medical University, Yenagoa, Bayelsa State, Nigeria

Corresponding authors:
Emmanuel B AttahDaniel, Environmental Fate of Chemicals and Remediation Laboratory, Department of Biotechnology and Chemistry, Vaal University of Technology, Bolivard Road, Vanderbijlpark, Gauteng 1911, South Africa.
Email: emmanuelabe@gmail.com

Paul N Diagboya, Environmental Fate of Chemicals and Remediation Laboratory, Department of Biotechnology and Chemistry, Vaal University of Technology, Bolivard Road, Vanderbijlpark, Gauteng, 1911, South Africa.
Email: pauldn2@yahoo.com

adsorption and may be tailored for higher adsorption efficiency.[2,3,6,7] These merits notwithstanding, most low-cost adsorbents suffer a lack of sufficient adsorption efficiency for water treatment while others are difficult to handle or separate from water post-treatment.

Recent advances in adsorption techniques suggest that synergistic combination of the functional properties of some low-cost adsorbents to form new composites may be employed to enhance adsorption efficiency (or capacity) and improve the ease of handling adsorbents (for instance by reducing bleeding or enhancing magnetic separation).[3,7,8] This technique has been employed to enhance low-cost adsorbents such as clays and biomasses composites[1,2,9–13] and mesoporous composite materials.[4,6,14–20] This approach has led to the preparation of other complex adsorbents such as the metal-organic framework (MOF)/platinum/activated carbon composite which was employed in the enhanced ($\approx$3 times) H_2 adsorption,[21] and the MOF/graphene oxide (GO) composite employed for the enhanced adsorption of dyes from wastewater.[22] Similarly, poly (vinyl alcohol) (PVA)/multiwall carbon-nanotube (MWCNT) composite was used for enhanced ($\geqslant$80%) aqueous Pb(II) sequestration from wastewater,[23] while PVA/poly(ethylene oxide) (PEO) hydrogel exhibited enhanced ($\approx$8 times) MB removal from dye wastewater.[24] In addition to the above, PEO is proving to be an efficient material in enhancing composites; for instance, GO/PEO nano-composite hydrogel adsorbent similarly exhibited effective removal of aqueous Cu(II).[25] Thus, PEO is proving to be an effective synergistic adsorbent.

The MOFs are an underutilized group of porous adsorbent; they are a class of porous crystalline materials with pore size and shape which are tunable via organic linker and inorganic moiety interaction.[26–29] Though MOFs can be tailored to express multiple enhanced adsorbent properties, recent reports suggest that MOFs may not exhibit excellent adsorption capacities and are actually difficult to remove from water post-treatment. Hydrogels on the other hand form massive insoluble 3D polymeric chain network via physical and chemical cross-linking and can possess the ability to adsorb contaminants with easy removal from water post-treatment.[30,31] Hence, synergistically combining MOFs and other materials, such as PEO hydrogel, may be an effective technique to improve the MOFs properties and enhance the adsorption capacity. Thus, this study reports a synergistically combined MOF and PEO adsorbent which was employed for the sequestration of MB from dye wastewater.

Materials and method

Materials and preparation of metal-organic framework and polyethylene oxide hydrogel

Ultra-pure water and analytical grade chemicals were used throughout this work. The chemicals used include lanthanum (III) nitrate hexahydrate ($LaN_3O_9.6H_2O$) (Merck), poly (ethylene oxide) (PEO) (Sigma Aldrich), poly(vinyl alcohol) (Sigma Aldrich), glutaraldehyde (Merck), N,N-Dimethylformamide ($HCON(CH_3)$) (AR) (Promark Chemicals), Methanol (CH_3OH) (99.99%) (Promark chemicals), terephthalic acid (1,4 benzene dicarboxylic acid) (Acros Organics), hydrochloric acid (Merck), nitric acid (Merck), and methylene blue ($C_{16}HClN_3S$) (Labochem).

Similar metal organic framework (MOF) preparation method as reported[32] was used for the preparation of lanthanum metal organic framework (LaBDC). The $LaN_3O_9.6H_2O$ (0.02008 mol) and terephthalic acid ($C_8H_6O_4$) (0.02008 mol) were dissolved in 80 mL of $HCON(CH_3)$ and refluxed under mild stirring for 8 h at 100°C. The MOF product of the reaction was centrifuged, washed with methanol thrice, oven dried at 75°C for 6 h, labeled LaBDC and preserved for further use.

Earlier hydrogel preparation methods reported[25,33] were adopted for the preparation of the PEO hydrogel. About 10.0 g of PVA polymer was dissolved in 100 mL of ultra-pure water in a 250 mL beaker at 90°C on a hot plate with mild stirring and cooled to room temperature, the PEO (5 mL) was added followed by 10 mL of 2.5% glutaraldehyde solution in 1% HCl, as a cross-linking agent and catalyst to the reaction mixture. This was stirred for 15 min and incubated at 80°C in an air ventilated oven. The hydrogel product was incubated in the oven at 80°C overnight to eliminate water then freeze dried, labeled PEO hydrogel and preserved for further use.

MOF-hydrogel (PEO-LaBDC) composite

The MOF-hydrogel (PEO-LaBDC) composite was prepared following earlier reported method.[25,33] A mass of 10.0 g of PVA polymer in a 250 mL beaker was dissolved in 100 mL of ultra-pure water at 90°C while stirring and allowed to cool to room temperature (24°C). A mass of 100 mg of LaBDC was then added to the cooled reaction mixture under vigorous stirring and 5 mL of PEO was added, followed by 10 mL of 2.5% glutaraldehyde solution in 1% HCl (cross-linking agent and catalyst) and vigorously stirred for 15 min (Figure 1). The reaction mixture was incubated and freeze dried as described above to produce the PEO-LaBDC composite hydrogel.

Characterization of the adsorbents

The physicochemical properties of the pristine LaBDC MOF, PEO hydrogel, and PEO-LaBDC composite were determined with the aid of a Zeiss Auriga Field Emission Scanning Electron Microscope (Germany) and Fourier Transform Infra-red spectrophotometer (Thermo Scientific, NICOLET iS50, USA). A T80 + UV-visible spectrometer was used for the determination
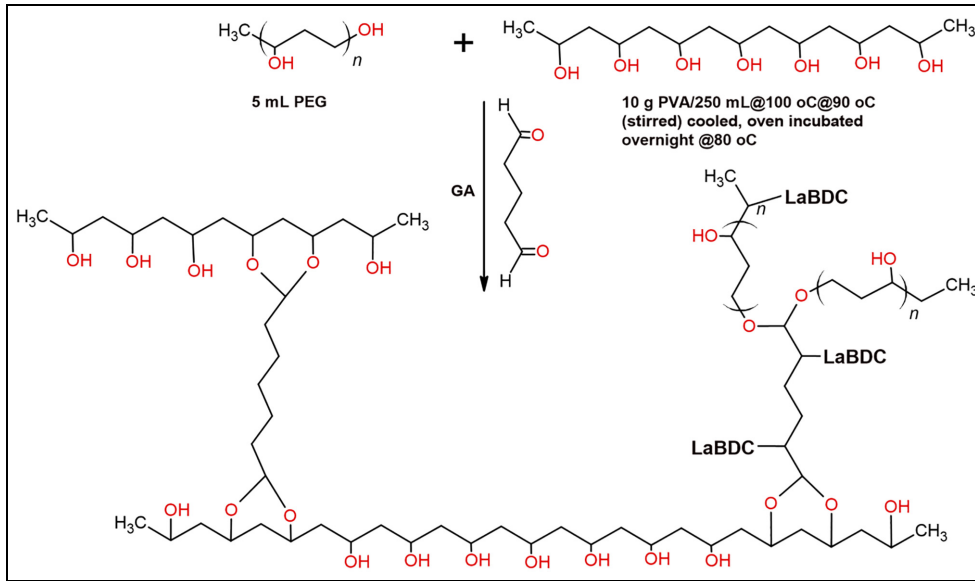
Figure 1. Schematics of the preparation of PEO-LaBDC composite.

of the residual concentration of MB from the batch adsorption experiments.

Batch adsorption studies using LaBDC, PEO hydrogel, and PEO-LaBDC composite

Adsorption kinetics studies and effect of pH on the MB adsorption were carried out using all adsorbents: LaBDC MOF, PEO hydrogel, and PEO-LaBDC composite. These experiments were carried out in duplicates for reproducibility. A stock solution of MB (1000 mg/L) was used to prepare the working solutions (20 mg/L) via serial dilution throughout this study. Batch adsorption studies of MB were carried out using 20 mg of LaBDC, PEO hydrogel, or PEO-LaBDC composite hydrogel in 20 mL of MB in 50 mL plastic tubes. An electric shaker at 200 rpm was used to equilibrate the mixtures of MB and each adsorbent per time. For the rate (effect of time) of MB adsorption, tubes representing varying time from 1 to 360 min were equilibrated and in due time, tubes representing specific times were retrieved from the shaker, centrifuged at 4000 rpm for 10 min and the supernatant was used to determine the concentration of MB left in the solution. The adsorption equilibrium times were recorded as 120 and 1 min for LaBDC and PEO hydrogel, respectively, while it was 60 min for the PEO-LaBDC composite hydrogel. Thus, the study of the effect of pH was carried out in the pH range of 4–12 using equilibrium time of 120, 1 and 60 min for LaBDC, PEO and PEO-LaBDC, respectively, while using 20 mL of MB solution (20 mg/L) and 20 mg of each adsorbent.

Data analysis

Equation (1) was used to evaluate the quantity, q_e (mg/g), of MB adsorbed by each of the adsorbents.

$$q_e = \frac{v}{m}(C_o - C_e) \tag{1}$$

where the initial and final concentrations of MB, the quantity of MB adsorbed in mg/g at equilibrium, volume of the solution (mL) and mass (g) of adsorbent used are denoted as C_o, C_e, q_e, v, and m, respectively.

The effect of time experimental data obtained for each of these adsorbents were subjected to further analysis using four non-linear kinetic models; the pseudo first order (PFO) (equation (2)), pseudo second order (PSO) (equation (3)), the homogeneous fractal pseudo second order (FPSO) (equation (4)) and the Webber-Morris intra particle diffusion kinetic (IPD) (equation (5)).[2,12]

$$q_t = q_e\left(1 - e^{-k_1 t}\right) \tag{2}$$

$$q_t = \frac{q_e^2 k_2 t}{1 + q_e k_2 t} \tag{3}$$

$$q_t = \frac{k_f q_e^2 t^\alpha}{1 + k_f q_e t^\alpha} \tag{4}$$

$$q_e = k_{IPD} t^{1/2} + C \tag{5}$$

The items q_e and q_t are the quantity of MB adsorbed (mg/g) at equilibrium and time t, respectively; and k_1 (/min) and k_2 (g/mg/min) are the rate constants of the PFO and PSO, respectively. The k_i (g/g/min$^{1/2}$) is the rate parameter of IPD control stage and C is the surface concentration of MB on each adsorbent. The Origin 8 pro software was used to generate all model parameters.
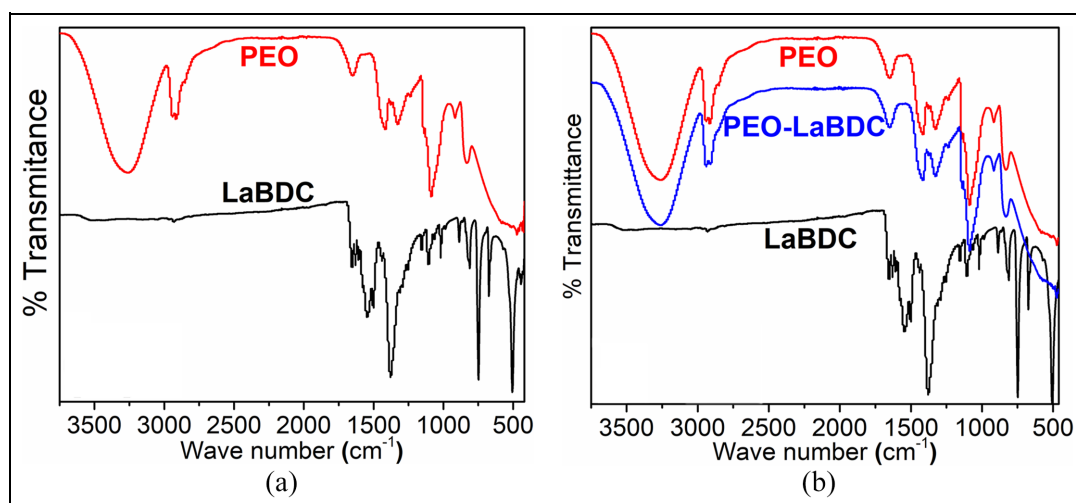
Figure 2. FTIR spectra of (a) LaBDC and PEO, and (b) LaBDC, PEO, PEO-LaBDC composite.

Results and discussions

Adsorbents' physicochemical properties

The FTIR spectra of the pristine LaBDC MOF, PEO hydrogel, and PEO-LaBDC composite are presented in Figure 2. The FTIR spectra (Figure 2(a)) of the pristine LaBDC MOF exhibited a broad peak at $3200\,cm^{-1}$ which was ascribed to $-OH$ stretching vibration.[6] The peaks at 1572, 1508, and $1421\,cm^{-1}$ were ascribed to vibrational modes of $–C=O$ typical to the carboxylate in the LaBDC, while the peak at $1277\,cm^{-1}$ was for the $C-H$ bending vibration. The spectra peaks exhibited at $1107.1\,cm^{-1}$ was due to $C-N$ stretching vibration from DMF[34,35] signifying that trace quantity of the DMF used for the synthesis occupied some pores of the pristine LaBDC. The sharp peak at $747\,cm^{-1}$ in the LaBDC spectrum was attributed to C-H bending vibration from the benzene ring[36] while the peak at $504.5\,cm^{-1}$ was attributed to the La-O bending vibrations.[35–37] The spectra of the PEO hydrogel (Figure 2(a)) revealed strong peaks of the functional groups present in the hydrogel. For instance, the stretching vibration peaks of $-OH$ in the cross linker were observed at $3257.9\,cm^{-1}$. The peaks at 2940.5 and $1087.6\,cm^{-1}$ (Figure 2(a)) were attributed to C-H and C-O stretching vibrations, respectively; both peaks were comparable to those earlier reported.[38] At $2941.0\,cm^{-1}$, the adsorption peaks obtained were ascribed to C-H bond of the CH_2 group of the PEO polymer.[33,39] The characteristic adsorption peaks of PEO hydrogel corresponding to C_6H_6 and C-O-C groups were observed at 1416.7 and $1327.6\,cm^{-1}$ for the PEO hydrogel.[40]

The PEO-LaBDC composite FTIR spectra (Figure 2(b)) exhibited a combination of peaks from both the PEO hydrogel and the LaBDC MOF (Figure 2(a)) though with slight shifts observed for some of the functional peaks in the composite. These shifts could be assumed to have resulted from the incorporation of LaBDC MOF in the PEO hydrogel matrix to obtain the PEO-LaBDC composite. Theoretically, peaks of the interacting functional groups are assumed to shift toward lower wave number.[25] In the PEO-LaBDC composite, the peak due to the stretching vibration mode of O-H group in the cross linker was observed at $3257.4\,cm^{-1}$ (Figure 2(b)), while the peaks at 2941.0 and $1087.0\,cm^{-1}$ (Figure 2(b)) were attributed to C-H and C-O stretching vibrations, respectively.[39] The adsorption peaks ascribed to the C-H bond of the composite-CH_2 group were found at $2941.0\,cm^{-1}$ similar to the spectra of PEO.[33] The $C=O$ stretching vibrations (assumed to be from the ester group formed within the composite) was expressed at $649.4\,cm^{-1}$, while the characteristic peaks of C_6H_6 and C-O-C groups were unchanged as those in the PEO hydrogel.[40]

The SEM micrographs of the pristine LaBDC, PEO hydrogel and PEO-LaBDC composite are shown in Figure 3. The micrographs indicated that the LaBDC had well defined cubic shape structures (Figure 3(a) and (b)). The morphology of the PEO hydrogels (Figure 3(c) and (d)) exhibited pores which resulted from syneresis (expulsion of moisture resulting in the cross-linking) for the formation of the PEO hydrogel. The PEO-LaBDC composite (Figure 3(e) and (f)) also exhibited the peculiarity to syneresis during hydrogel formation creating smaller pores in the hydrogel from the crosslinking and loading of LaBDC MOF into the PEO matrix. The pores on the PEO-LaBDC (Figure 3(e) and (f)) composite on very close physical inspection of the SEM micrographs appear to be more closely positioned than in the PEO which might have resulted from the linkage between the pristine LaBDC MOF and the pristine PEO to form the PEO-LaBDC composite. Syneresis facilitated the approximation of the polymer chains to form the hydrogel during cross-linking leading to reduction in the structure. The extrusion of moisture as droplets from the hydrogel network also contributed to the formation of pores.[24]
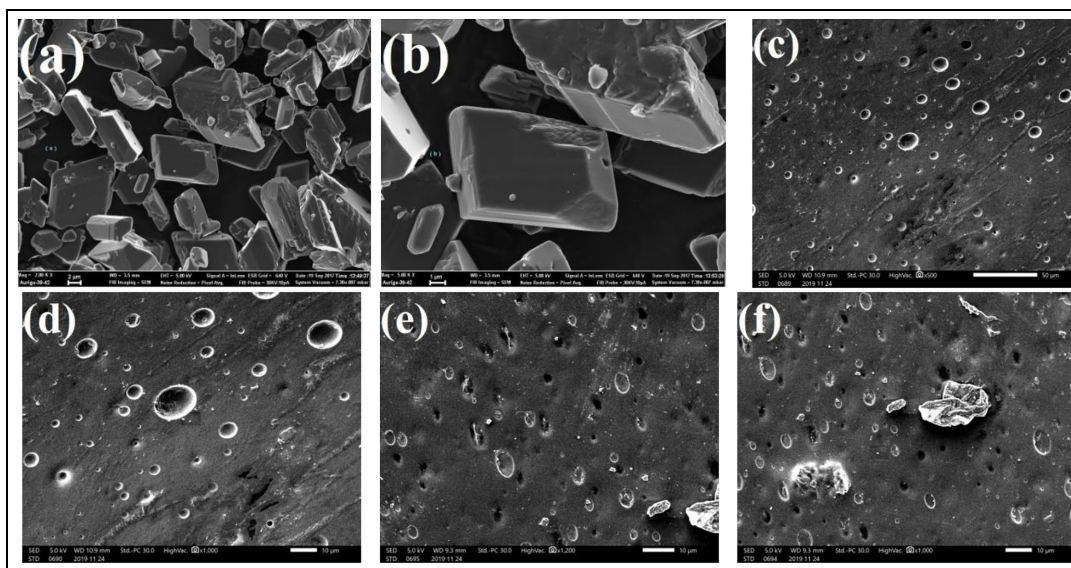
Figure 3. Scanning Electron Microscope images of bricked shaped LaBDC MOF (a and b); PEO hydrogel (c and d); and PEO-LaBDC composite (e and f).
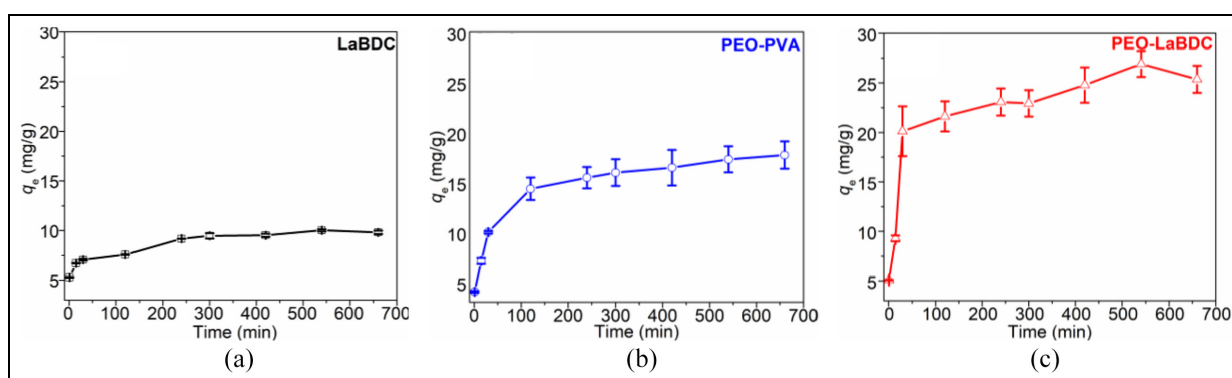

Figure 4. Adsorption rates of MB at varying time for (a) LaBDC, (b) PEO, and (c) PEO/LaBDC composite.

Dye uptake studies and data analysis

Kinetics of MB adsorption on the LaBDC, PEO and PEO-LaBDC. Adsorption experiments were carried out on pristine LaBDC MOF, PEO, and PEO-LaBDC adsorbents to determine the uptake rate. The adsorption trends (Figure 4(a)–(c)) showed an increased uptake with time; this was ascribed to the availability of adsorption sites for the cationic MB. The MB uptake of all adsorbents increased with time until the adsorption sites were filled and the curves in Figure 4 became plateaus which marked equilibrium time.[14,15] At equilibrium, the various adsorption rates expressed insignificant differences between uptake and desorption.[2,41] The trends showed that the equilibrium time of removal of MB by the pristine LaBDC MOF was 120 min (Figure 4(a)), PEO hydrogel (Figure 4(b)) was slower with equilibrium time of 125 min when compared to the pristine LaBDC MOF and the composite (PEO-LaBDC) (Figure 4(c)) was faster and reached equilibrium within 60 min. Thus, the composite exhibited a faster rate of adsorption than either of the pristine adsorbents, hence a better adsorbent.

Insights into the adsorption mechanisms were obtained by employing the experimental data through fitting into four non-linear kinetic models: PFO, PSO, FPSO and the Webber-Morris IPD (Table 1). Comparing the generated model data of the PFO, PSO and FPSO suggested that the FPSO fitted the adsorption data better with higher correlation coefficients ($r^2 \geqslant 0.796$), smaller chi square (χ^2), and with q_e values closer to experimental values; and this model could sufficiently describe the mechanism of MB uptake from solution by these adsorbents. Though the estimated FPSO q_e value for LaBDC was significantly higher than the experimental value, other parameters suggested the sorption process could be described by the FPSO. The FPSO model implied that the adsorption processes were complex and that electrostatic
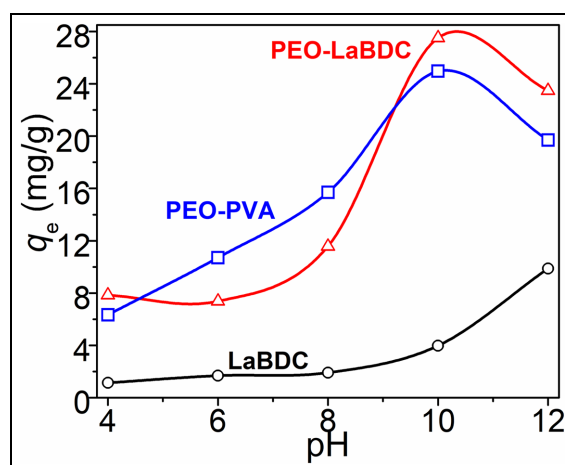
Table 1. The values of the respective kinetics model parameters used for the evaluation of MB adsorption.

Kinetic model	Parameter	LaBDC	PEO-PVA	PEO/LaBDC
PFO	r^2	0.411	0.885	0.888
	χ^2	1.704	2.769	6.667
	q_e(mg/g)	8.8	16.2	24.6
	K_1	0.911	0.034	0.043
PSO	r^2	0.532	0.927	0.901
	χ^2	1.354	1.747	5.877
	q_e(mg/g)	9.0	17.4	26.1
	K_2	0.122	0.002	0.002
FPSO	r^2	0.991	0.984	0.905
	χ^2	0.024	0.392	5.621
	K_f	4.7×10^{-4}	0.005	0.005
	q_e(mg/g)	106.5	25.7	30.0
	ö	0.114	0.415	0.582
IPD	r^2	0.918	0.873	0.749
	χ^2	0.237	3.067	14.917
	K_{IPD}	0.184	0.521	0.767
	C (mg/g)	5.9	6.0	9.6

Figure 5. Effect of pH on adsorption of MB by LaBDC, PEO hydrogel, and PEO-LaBDC composite.

interactions and other Vander Waals forces were involved in the uptake of MB molecules from solution during the adsorption process.[13]

Evaluation of the experimental data fitting of the Webber-Morris IPD model showed that the LaBDC adsorbent exhibited a relatively high surface adsorption (C) of 5.9 mg/g ($\approx$60%) compared to the PEO having $\approx$6.0 mg/g ($\approx$34%) surface adsorption. Subtracting the surface adsorption from total adsorption, the rest were attributed to adsorption within the pores of the adsorbents.[20] The observed IPD model results of the composite PEO-LaBDC showed that the composite surface adsorption were somewhat in between those of both pristine materials.

Effect of pH on MB adsorption onto LaBDC, PEO hydrogel and PEO-LaBDC composite. The effect of the adsorbate (MB) solution pH on adsorption was studied between pH 4 and 12 since pH affects the charge densities surrounding the adsorbent and adsorbate in solution.[9,42] The trend observed showed that at lower pH the three adsorbents demonstrated low uptake of MB (Figure 5), but as the pH increased, a corresponding increase in the MB uptake was observed which reached optimum at the alkaline pH region for all adsorbents. The pH of optimum adsorption was observed to be 12, 10, and 10 for the LaBDC, PEO hydrogel and PEO-LaBDC composite, respectively, with optimum MB adsorption of 9.1, 17.0, and 27.3 mg/g accordingly. Comparatively, the composite exhibited a better adsorption performance; buttressing the idea that synergism between adsorbents could enhance adsorption processes. The adsorption trend as pH increased implied that the surfaces of these adsorbents as well as the MB were highly

protonated (H^+) and uncharged at low pH which resulted in reduced electrostatic interactions between the adsorption sites and the cationic MB molecules, hence the reduced adsorption. However as the ambient solution pH increased from pH 4 toward alkalinity, the proton concentration in the solution decreased continuously resulting in deprotonation of the adsorption surfaces and the MB molecules with a consequent buildup of electrostatic attraction between both surfaces.[41] This was what led to the enhanced adsorption of cationic MB observed.[43–46]

Comparative examination of the optimum adsorption of all three adsorbents studied at varying solution pH showed that the PEO-LaBDC composite exhibited the highest MB uptake (27.5 mg/g) at pH 10 which accounts for $\approx$177% increase in adsorption when compared with the pristine LaBDC MOF (9.1 mg/g) at optimum adsorption pH of 12. Thus, this result supports the trends in recent reports that synergistic combination of adsorbents in composite materials is one way to enhance the adsorptive removal of pollutants in aqueous media. Therefore, the PEO-LaBDC composite is a promising adsorbent for the remediation of MB from aqueous media.

Conclusion

A synergistic adsorbent, PEO-LaBDC composite was prepared from pristine LaBDC MOF and PEO hydrogel. The pristine and composite adsorbents were successfully characterized and employed for MB adsorption from aqueous solution. The composite exhibited a faster rate of adsorption than either of the pristine adsorbents, hence a better adsorbent, and the kinetics followed the FPSO model. The PEO-LaBDC exhibited $\approx$177% increase in adsorption when compared with the pristine LaBDC MOF at optimum adsorption pH; thus, the PEO-LaBDC composite is a

potential effective adsorbent for the removal of MB from dye contaminated water.

Author's note

PN Diagboya is a visiting scientist at Institute of Soil Science and Soil Conservation, Justus Liebig University, Gießen, Germany

Declaration of conflicting interests

The author(s) declared no potential conflicts of interest with respect to the research, authorship, and/or publication of this article.

ORCID iD

Paul N Diagboya https://orcid.org/0000-0003-2982-433X

Data availability statement

Data are available from the corresponding author upon reasonable request.

References

1. Olu-Owolabi BI, Alabi AH, Diagboya PN, et al. Adsorptive removal of 2,4,6-trichlorophenol in aqueous solution using calcined kaolinite-biomass composites. *J Environ Manag* 2017; 192: 94–99.
2. Sera PR, Diagboya PN, Akpotu SO, et al. Potential of valourized Moringa oleifera seed waste modified with activated carbon for toxic metals decontamination in conventional water treatment. *Bioresour Technol Rep* 2021; 16: 100881.
3. Diagboya PN, Olu-Owolabi BI, Mtunzi FM, et al. Clay-carbonaceous material composites: towards a new class of functional adsorbents for water treatment. *Surf Interfaces* 2020; 19: 100506.
4. Diagboya PN, Olu-Owolabi BI, Zhou D, et al. Graphene oxide–tripolyphosphate hybrid used as a potent sorbent for cationic dyes. *Carbon N Y* 2014; 79: 174–182.
5. Onkani SP, Diagboya PN, Mtunzi FM, et al. Comparative study of the photocatalytic degradation of 2-chlorophenol under UV irradiation using pristine and Ag-doped species of $TiO(2)$, ZnO and ZnS photocatalysts. *J Environ Manag* 2020; 260: 110145.
6. Zanele ZP, Mtunzi FM, Nelana SM, et al. Metals and antibiotics as aqueous sequestration targets for magnetic polyamidoamine-grafted SBA-15. *Langmuir* 2021; 37: 9764–9773.
7. Diagboya PNE and Dikio ED. Silica-based mesoporous materials; emerging designer adsorbents for aqueous pollutants removal and water treatment. *Microporous Mesoporous Mater* 2018; 266: 252–267.
8. Akpotu SO, Lawal IA, Diagboya PN, et al. Engineered geomedia kaolin clay-reduced graphene oxide-polymer composite for the remediation of olaquindox from water. *ACS Omega* 2022; 7: 34054–34065.
9. Diagboya PN and Dikio ED. Scavenging of aqueous toxic organic and inorganic cations using novel facile magneto-carbon black-clay composite adsorbent. *J Clean Prod* 2018; 180: 71–80.
10. Mohubedu RP, Diagboya PNE, Abasi CY, et al. Magnetic valorization of biomass and biochar of a typical plant nuisance for toxic metals contaminated water treatment. *J Clean Prod* 2019; 209: 1016–1024.
11. Olu-Owolabi BI, Alabi AH, Unuabonah EI, et al. Calcined biomass-modified bentonite clay for removal of aqueous metal ions. *J Environ Chem Eng* 2016; 4: 1376–1382.
12. Olu-Owolabi BI, Diagboya PN, Mtunzi FM, et al. Utilizing eco-friendly kaolinite-biochar composite adsorbent for removal of ivermectin in aqueous media. *J Environ Manag* 2021; 279: 111619.
13. Olu-Owolabi BI, Diagboya PN, Unuabonah EI, et al. Fractal-like concepts for evaluation of toxic metals adsorption efficiency of feldspar-biomass composites. *J Clean Prod* 2018; 171: 884–891.
14. Diagboya PN, Mmako HK, Dikio ED, et al. Synthesis of amine and thiol dual functionalized graphene oxide for aqueous sequestration of lead. *J Environ Chem Eng* 2019; 7: 103461.
15. Diagboya PN, Mtunzi FM, Düring R-A, et al. Empirical assessment and reusability of an eco-friendly amine-functionalized SBA-15 adsorbent for aqueous ivermectin. *Ind Eng Chem Res* 2021; 60: 2365–2373.
16. Diagboya PN, Olu-Owolabi BI and Adebowale KO. Microscale scavenging of pentachlorophenol in water using amine and tripolyphosphate-grafted SBA-15 silica: batch and modeling studies. *J Environ Manag* 2014; 146: 42–49.
17. Diagboya PN, Olu-Owolabi BI and Adebowale KO. Synthesis of covalently bonded graphene oxide–iron magnetic nanoparticles and the kinetics of mercury removal. *RSC Adv* 2015; 5: 2536–2542.
18. Ebelegi AN, Ayawei N, Wankasi D, et al. Covalently bonded polyamidoamine functionalized silica used as a Pb(II) scavenger from aqueous solution. *J Environ Chem Eng* 2019; 7: 103214.
19. Mtunzi FM, Diagboya PN, Düring R-A, et al. Mesoporous SBA-15 functionalized with G-5 polyamidoamine: a sustainable adsorbent for effective sequestration of an emerging aqueous contaminant. *ACS Appl Nano Mater* 2021; 4: 3052–3061.
20. Xikhongelo RV, Mtunzi FM, Diagboya PN, et al. Polyamidoamine-functionalized graphene Oxide–SBA-15 mesoporous composite: adsorbent for aqueous arsenite, cadmium, ciprofloxacin, ivermectin, and tetracycline. *Ind Eng Chem Res* 2021; 60: 3957–3968.
21. Sumida K, Hill MR, Horike S, et al. Synthesis and hydrogen storage properties of $Be_{12}(OH)_{12}(1,3,5\text{-benzenetribenzoate})_4$. *J Am Chem Soc* 2009; 131: 15120–15121.
22. Zhang Y, Tao CA, Song J, et al. Metal-organic frameworks/graphene oxide composites: preparation and applications in dye absorption. In: *4th ICSEEE*, 2015, pp.642–645. New York, NY: IEEE.
23. Abraham TN, Kumar R, Misra RK, et al. Poly(vinyl alcohol)-based MWCNT hydrogel for lead ion removal from contaminated water. *J Appl Polym Sci* 2012; 125: E670–E674.

24. Teixeira RSP, Correa RJ, Bello Forero JS, et al. Comparative study of PEO and PVA hydrogels for removal of methylene blue dye from wastewater. *J Appl Polym Sci* 2017; 134: 45043.

25. Serag E, El Nemr A and El-Maghraby A. Synthesis of highly effective novel graphene oxide-polyethylene glycol-polyvinyl alcohol nanocomposite hydrogel for copper removal. *J Water Environ Nanotechnol* 2017; 2: 223–234.

26. Yaghi OM, O'Keeffe M, Ockwig NW, et al. Reticular synthesis and the design of new materials. *Nature* 2003; 423: 705–714.

27. Farrusseng D, Aguado S and Pinel C. Metal-organic frameworks: opportunities for catalysis. *Angew Chem Int Ed* 2009; 48: 7502–7513.

28. Lee J, Farha OK, Roberts J, et al. Metal-organic framework materials as catalysts. *Chem Soc Rev* 2009; 38: 1450–1459.

29. Wang H, Jia S, Wang H, et al. A novel-green adsorbent based on betaine-modified magnetic nanoparticles for removal of methyl blue. *Sci Bull* 2017; 62: 319–325.

30. Zaman M, Siddique W, Waheed S, et al. Hydrogels, their applications and polymers used for hydrogels: a review. *Int J Biol Pharm Allied Sci* 2015; 4: 6581–6603.

31. Ganji F, Vasheghani FS and Vasheghani FE. Theoretical description of hydrogel swelling: a review, *Iran Polym J* 2010; 19:375–398.

32. Shooto ND, Ayawei N, Wankasi D, et al. Study on cobalt metal organic framework material as adsorbent for lead ions removal in aqueous solution. *Asian J Chem* 2016; 28: 277–281.

33. Serag E, El Nemr A, Fathy SA, et al. A novel three dimensional carbon nanotube-polyethylene glycol-Polyvinyl alcohol nanocomposite for Cu(II) removal from water. *Egypt J Aquat Biol Fish* 2018; 22: 103–118.

34. Zhu B-J, Yu X-Y, Jia Y, et al. Iron and 1,3,5-benzenetricarboxylic metal–organic coordination polymers prepared by solvothermal method and their application in efficient As(V) removal from aqueous solutions. *J Phys Chem C* 2012; 116: 8601–8607.

35. Prabhu SM, Imamura S and Sasaki K. Mono-, Di-, and tricarboxylic acid facilitated lanthanum-based organic frameworks: insights into the structural stability and mechanistic approach for superior adsorption of arsenate from water. *ACS Sustain Chem Eng* 2019; 7: 6917–6928.

36. Chen M, Huo C, Li Y, et al. Selective adsorption and efficient removal of phosphate from aqueous medium with graphene–lanthanum composite. *ACS Sustain Chem Eng* 2016; 4: 1296–1302.

37. Hosseini S, Paymanfar R, Afshari T, et al. Preparation of MWCNT/Ba0.2Sr0.2La0.6MnO3/PANI nanocomposites and investigation of its electromagnetic properties in KU-band. *Int J Phys Sci* 2020; 15: 171–181.

38. Abu Ghalia M and Dahman Y. Radiation crosslinking polymerization of poly (vinyl alcohol) and poly (ethylene glycol) with controlled drug release. *J Polym Res* 2015; 22: 1–9.

39. Diagboya PN and Dikio ED. Dynamics of mercury solid phase extraction using Barbula lambarenensis. *Environ Technol Innov* 2018; 9: 275–284.

40. Falqi FH, Bin-Dahman OA, Hussain M, et al. Preparation of miscible PVA/PEG blends and effect of graphene concentration on thermal, crystallization, morphological, and mechanical properties of PVA/PEG (10 wt%) blend. *Int J Polym Sci* 2018; 2018: 1–10.

41. Diagboya PN, Mtunzi FM, Adebowale KO, et al. Comparative empirical evaluation of the aqueous adsorptive sequestration potential of low-cost feldspar-biochar composites for ivermectin. *Colloids Surf A Physicochem Eng Asp* 2022; 634: 127930.

42. Nkutha CS, Diagboya PN, Mtunzi FM, et al. Application of eco-friendly multifunctional porous graphene oxide for adsorptive sequestration of chromium in aqueous solution. *Water Environ Res* 2020; 92: 1070–1079.

43. Abasi CY, Diagboya PNE and Dikio ED. Layered double hydroxide of cobalt-zinc-aluminium intercalated with carbonate ion: preparation and Pb(II) ion removal capacity. *Int J Environ Stud* 2019; 76: 251–265.

44. Fallah Shojaei A, Tabatabaeian K and Zebardast M. Ferric ion modified nano-MOF-5 synthesized by direct mixing approach: a highly efficient adsorbent for methylene blue dye. *Sci Iran* 2018; 25: 1323–1334.

45. Khodaie M, Ghasemi N, Moradi B, et al. Removal of methylene blue from wastewater by adsorption onto ZnCl$_2$Activated corn husk carbon equilibrium studies. *J Chem* 2013; 2013: 1–6.

46. Konicki W and Pełech I. Removing cationic dye from aqueous solutions using as-grown and modified multi-walled carbon nanotubes. *Pol J Environ Stud* 2018; 28: 717–727.